

Winding Loss Calculation with Multiple Windings, Arbitrary Waveforms and Two-Dimensional Field Geometry

C. R. Sullivan

Found in *IEEE Industry Applications Society Annual Meeting*, Oct. 1999, pp. 2093–2099.

©1999 IEEE. Personal use of this material is permitted. However, permission to reprint or republish this material for advertising or promotional purposes or for creating new collective works for resale or redistribution to servers or lists, or to reuse any copyrighted component of this work in other works must be obtained from the IEEE.

Winding Loss Calculation with Multiple Windings, Arbitrary Waveforms, and Two-Dimensional Field Geometry

Charles R. Sullivan

Thayer School of Engineering

8000 Cummings Hall, Dartmouth College, Hanover, NH 03755-8000

charles.r.sullivan@dartmouth.edu

603-643-2477

<http://engineering.dartmouth.edu/inductor>

Abstract-- A method for calculating eddy-current (proximity-effect) losses in transformer and inductor windings is introduced. The new method is capable of analyzing losses due to two- and three-dimensional field effects in multiple windings with arbitrary waveforms in each winding. It uses a simple set of numerical magnetostatic field calculations to derive a matrix describing the transformer or inductor. This is combined with a second matrix calculated from derivatives of winding currents to computer total ac loss. Experiments show the method is accurate for coils that are not in or close to self-resonance.

I. INTRODUCTION

Magnetic component performance is essential for high-frequency power conversion; often the magnetic components are the most expensive and largest parts of a system, and can pose some of the most severe loss and thermal problems. Circuit designs are often predicated on minimizing requirements for magnetic components. Despite the importance of magnetic components, the state of the art in magnetic component design leaves much to be desired. In particular, standard methods of analyzing winding loss [1-18] ([16] gives a useful review) assume a one-dimensional field for analyzing eddy-current effects in windings. But two-dimensional effects are important in any magnetic component that includes a discrete air gap. In this paper, we introduce a new method that includes the effects of two- or three-dimensional fields, while taking into account multiple windings and non-sinusoidal waveforms that may be different in each winding. The method applies to round-wire windings, including litz-wire windings.

A. Review of Previous Analytical Approaches

Although different descriptions can be used, most existing analytical calculations of high-frequency winding loss are fundamentally equivalent to one of three analyses. The most rigorous approach uses an exact calculation of losses in a cylindrical conductor with a known current, subjected to a uniform external field, combined with an expression for the field as a function of one-dimensional position in the winding area [6, 18]. Perhaps the most commonly cited analysis [7] uses "equivalent" rectangular conductors to approximate round wires, and then pro-

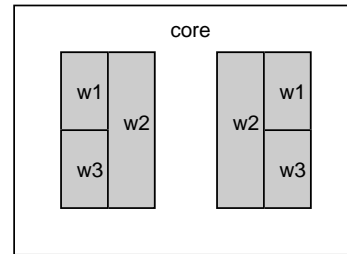


Fig. 1. Three-winding transformer (w1-w3) in which two-dimensional field geometry is important.

ceeds with an exact one-dimensional solution. Finally, one may use only the first terms of a series expansion of these solutions, e.g. [15, 19, 20].

For designs in which one-dimensional field analysis is accurate, and where wire strands are small compared to a skin-depth, these various methods are approximately equivalent [6], despite one small discrepancy explained in [21]. Although the basic analysis is usually based on sinusoidal waveforms, a number of authors have developed methods of extending this analysis to non-sinusoidal waveforms through Fourier analysis or other methods [11, 13, 19, 20, 21, 22, 23].

A major limitation of all of this work is that it does not apply to components in which the field geometry is not one-dimensional. This includes nearly all inductors and gapped transformers, in which the two-dimensional field geometry due to the gap significantly affects losses [24]. Standard one-dimensional analysis is also unable to analyze transformers with two-dimensional winding layout, such as the one shown in Fig. 1. In [25] an analytical approach is developed for two-dimensional fields in gapped single-winding inductors. Although this is an important accomplishment, the results are too complex for routine design work, they are specific to one geometry, and they do not account for multiple windings or arbitrary waveforms.

B. Limitations of General Purpose Electromagnetic Analysis

Work in computational electromagnetics has produced general-purpose field analysis methods, and commercial software is available for two and three-dimensional solutions of arbitrary problems, including analysis of eddy currents. However, there are two major limitations of this approach for high-frequency magnetics in power electronics applications.

- *Scale Problems*

The first limitation is a scale problem. Transformers and inductors often require many turns of fine wire, or may use stranded wire such as litz wire to reduce eddy current losses. The wire strands may be as small as 30-50 μm in diameter (44-48 AWG), while the overall dimensions may be tens of centimeters. Thus, the length scales involved can vary over two to four orders of magnitude, and there may be as many as 10,000 or more strands of wire. Even when larger wire is used, the skin depth in the wire can be small, for example 100 μm at 400 kHz, which creates the same problem. This leads to a need for a large number of elements in finite element analysis, and thus slow simulations and large memory requirements. To circumvent this problem, software vendors recommend modeling a stranded winding as a region of uniform current density. While this is helpful for analyzing field distributions, it provides no information on losses in the stranded winding.

- *Optimization*

With existing field analysis, optimization must be done by trial and error. Particularly when each iteration takes hours to analyze via finite element analysis, true optimization is not practical, except in a few academic experiments, which then provide information about only one particular design.

II. NEW ANALYSIS METHOD

In order to circumvent both the limitations of one-dimensional analytical methods, and the limitations of existing numerical methods, we use a combination of numerical calculation of the overall field geometry, with analytical calculation of its interaction with the winding strands. This avoids the scale problem, but allows applying the power of modern computers to quickly obtain a much more accurate solution than would be available through one-dimensional analysis. A similar approach was reported in [26] for gapped single-winding inductors with sinusoidal waveforms. The method we report here is more powerful, in that it is capable of analyzing

multi-winding transformers with different non-sinusoidal waveforms in each winding.

We start with the calculation of loss in a conducting cylinder in a uniform field, perpendicular to the axis of the cylinder, with the assumption that the field remains constant inside the conductor, equivalent to the assumption that the diameter is small compared to a skin depth. This results in instantaneous power dissipation $P(t)$ in a wire of length ℓ [19]

$$P(t) = \frac{\pi \ell d_c^4}{64 \rho_c} \left(\frac{dB}{dt} \right)^2, \quad (1)$$

where B is the flux density, ρ_c is the resistivity of the wire, and d_c is its diameter. The average loss depends on the time average of the squared derivative of the field, $\overline{\left(\frac{dB}{dt} \right)^2}$. We can also use the spatial average of this quantity to calculate the time average of total ac loss in a winding

$$P_{winding} = \frac{\pi \ell_{t,j} N_j d_{c,j}^4}{64 \rho_c} \overline{\left\langle \left(\frac{dB}{dt} \right)^2 \right\rangle_j} \quad (2)$$

where N_j is the number of turns in winding j , $\ell_{t,j}$ is the average length of a turn, $\langle \cdot \rangle_j$ indicates a spatial average over the region of winding j , and $\overline{\cdot}$ indicates a time average. For a litz-wire winding, the same expression may be used to calculate strand-level proximity-effect loss. In this case, N_j must represent the product of the number of turns and the number of strands in each turn (i.e., N_j is the total number of strands in the winding), and d_c is the diameter of the individual strands. The length of a turn may also need to be adjusted to account for the increased distance that a strand travels on account of twisting. This calculation neglects bundle-level effects, but this is usually valid because with proper bundle construction, they can be made negligible [21].

In a given winding, the field, \vec{B} may be expressed as the superposition of fields due to currents in each winding. We can then express the loss in winding j of a two-winding transformer as

$$P_{loss,j} = \gamma_j \overline{\left\langle \left(\frac{d\vec{B}_1}{dt} \right)^2 + \left(\frac{d\vec{B}_1}{dt} \right) \left(\frac{d\vec{B}_2}{dt} \right) + \left(\frac{d\vec{B}_2}{dt} \right) \left(\frac{d\vec{B}_1}{dt} \right) + \left(\frac{d\vec{B}_2}{dt} \right)^2 \right\rangle_j} \quad (3)$$

where $\gamma_j = \frac{\pi N_j \ell_{t,j} d_{c,j}^4}{64 \rho_c}$ and \vec{B}_k is the field due to current in winding k . We can express this in terms of the currents as

$$P_{loss,j} = a_{j,11} \overline{\left\langle \left(\frac{di_1}{dt} \right)^2 \right\rangle} + a_{j,12} \overline{\left\langle \frac{di_1}{dt} \frac{di_2}{dt} \right\rangle} + a_{j,21} \overline{\left\langle \frac{di_2}{dt} \frac{di_1}{dt} \right\rangle} + a_{j,22} \overline{\left\langle \left(\frac{di_2}{dt} \right)^2 \right\rangle} \quad (4)$$

where $a_{j,mn}$ is a constant relating current and loss, to be calculated in the next section. The total ac loss in all

windings is the sum of such terms for each winding, and can be expressed as

$$P_{loss,total} = \left[\frac{di_1}{dt} \quad \frac{di_2}{dt} \right] \mathbf{D} \begin{bmatrix} \frac{di_1}{dt} \\ \frac{di_2}{dt} \end{bmatrix} \quad (5)$$

where \mathbf{D} is the sum of the matrices a_{mn} for each winding,

$$\mathbf{D} = \sum_j a_{j,mn}. \quad (6)$$

\mathbf{D} can be termed a dynamic resistance matrix, comprising self-resistance and mutual resistance terms. It has units of $\Omega\text{-s}^2$.

An advantage of this formulation is that the matrix \mathbf{D} may be easily calculated from a set of magnetostatic field calculations for the transformer geometry (see the following section), and the matrix

$$\left[\frac{di_1}{dt} \quad \frac{di_2}{dt} \right] \begin{bmatrix} \frac{di_1}{dt} \\ \frac{di_2}{dt} \end{bmatrix} \quad (7)$$

may be easily calculated for the particular set of waveforms of interest. Then the inner product of these two matrices yields the total ac loss. To calculate total transformer loss, one must combine this figure with core loss and winding loss due to dc winding resistance ($R_{dc} I_{rms}^2$).

This analysis may be extended in the obvious way to an arbitrary number of windings, and is shown above for two windings only to simplify the presentation.

III. FIELD CALCULATIONS

The matrix \mathbf{D} needed for the above loss calculation can be shown to be

$$\mathbf{D} = \gamma_1 \left\langle \begin{bmatrix} \tilde{B}_1^2 & \tilde{B}_1 \tilde{B}_2 \\ \tilde{B}_2 \tilde{B}_1 & \tilde{B}_2^2 \end{bmatrix} \right\rangle_1 + \gamma_2 \left\langle \begin{bmatrix} \tilde{B}_1^2 & \tilde{B}_1 \tilde{B}_2 \\ \tilde{B}_2 \tilde{B}_1 & \tilde{B}_1^2 \end{bmatrix} \right\rangle_2 \quad (8)$$

where \tilde{B}_j is the field everywhere due to a unit current in winding j , and $\langle \cdot \rangle_j$ is the spatial average over the region of winding j . In order to find this we may calculate the fields due to current in each winding in turn. Then the quantities $\langle \tilde{B}_j^2 \rangle_k$ and $\langle \tilde{B}_j \tilde{B}_k \rangle_m$ may be calculated from these fields.

The field calculations may be done using any magnetostatic finite element analysis program, or by specialized methods that are more efficient for a particular problem, such as those discussed in [26]. Depending on the geometry involved and the accuracy required, the calculation may be two-dimensional (in Cartesian or cylindrical coordinates) or three-dimensional. In the three-dimensional

case, the field may not always be perpendicular to the axis of the wire, resulting in slightly lower loss in practice than the calculations presented here would predict. Although a correction for this could be made, in most cases this effect is not expected to be significant.

Irrespective of the field calculation method, the approach we have described for finding the value of \mathbf{D} entails calculating and storing the complete field information $\tilde{B}_1(\vec{x})$ and $\tilde{B}_2(\vec{x})$, and then finding the spatial averages of the square terms and of the cross products. An alternative that requires less data storage and may be more convenient with the user interfaces of some commercial finite element packages is to calculate the field with current in each winding individually, perform the necessary averages, and then calculate the field with current in both windings, repeat the averaging, and subtract to find the cross terms.

IV. VERIFICATION

The method has been tested with the transformer design shown in Table I. The design was chosen because of the significant two-dimensional effects produced by the gap and the winding design shown in Fig. 2, and because of the large number of strands (over 2500 total) in the winding window, which makes direct simulation prohibitive. The transformer was tested and analyzed with a gapped ferrite core and without a core. In the gapped core, large gaps (1 mm gaps in the centerpost and outer core legs) were used to minimize core loss effects. Although long gaps might intuitively seem to magnify the effect of gap fringing fields on ac resistance, longer gaps actually slightly decrease the effect [26, 27]. Thus, in the configuration we measured, the effect of gap fringing field on loss is slightly milder than in a typical practical design, but is still quite significant, as shown below.

TABLE I
TRANSFORMER USED FOR VERIFICATION

Windings		
N	Number of turns	162:162
p	Number of layers in each winding	2.5
	Wire type	8/36 litz
n	Number of strands in each turn	8
	Strand gauge	36 AWG
Core (used in some tests)		
Geometry	Round-center-post EE	ETD39
Material	MnZn Ferrite	TDK PC40
Gap	Centerpost and outer legs	1 mm
		(2 mm total)

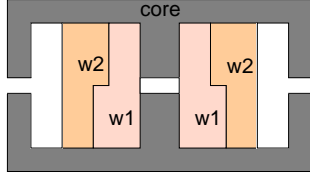


Fig. 2. Winding configuration tested, not to scale.

A. Field Calculations

Three magnetostatic simulations with a commercial finite element package [28] were used to find the field values with current in each winding individually, and with current in both simultaneously. The windings have cylindrical symmetry, and so for the air-core case an axisymmetric finite element simulation could be used to find the matrix \mathbf{D} . For the gapped ferrite core, three-dimensional magnetostatic simulations were used to account for the full three-dimensional geometry. The software's post-processor was used to find the average values of B^2 in each winding region, so that \mathbf{D} could be calculated as described in Section III.

B. Measurements

With the matrix \mathbf{D} , the loss could be predicted for any waveforms. However, accurate measurements could be most easily obtained for sinusoidal waveforms, using an HP 4284A impedance analyzer. Verifying the effect of each term in the matrix \mathbf{D} was possible by using different combinations of current in different windings: each driven individually, and both driven in series with the same or opposite polarities (exciting the magnetizing or leakage inductance, respectively).

Measurements of the real part of the impedance for each of these four configurations for the air-core transformer are shown in Fig. 3, along with predicted ac resistance from (5). Fig. 4 shows the corresponding data for the gapped core. Although the trends are correctly predicted in both cases, the results show substantial deviations at high frequencies, especially for the ferrite core. Other effects on the impedance were studied to determine the sources of these discrepancies.

C. Other Effects on Impedance

Core loss is one possible source of error for the measurement with a core. Core loss was measured with the two-winding technique on an ungapped core, at the same flux level used in the winding measurements. This correction had a minor effect improving the results, which is not a surprising result given the large gap length.

A more significant source of discrepancies is capacitive effects. This is to be expected based on the low self-

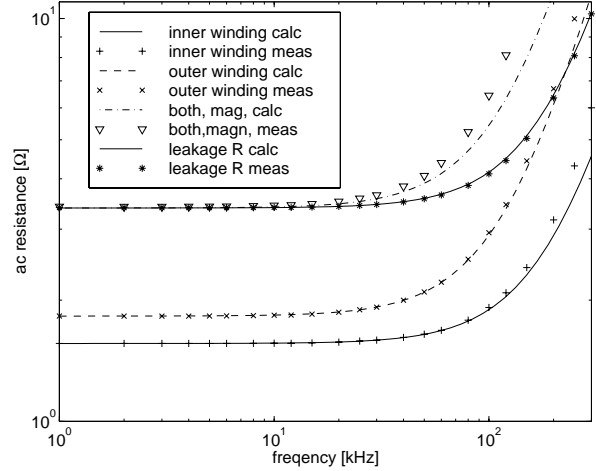


Fig. 3. Real part of the impedance of various winding configurations for the tested air-core coil, compared to the predicted ac resistance.

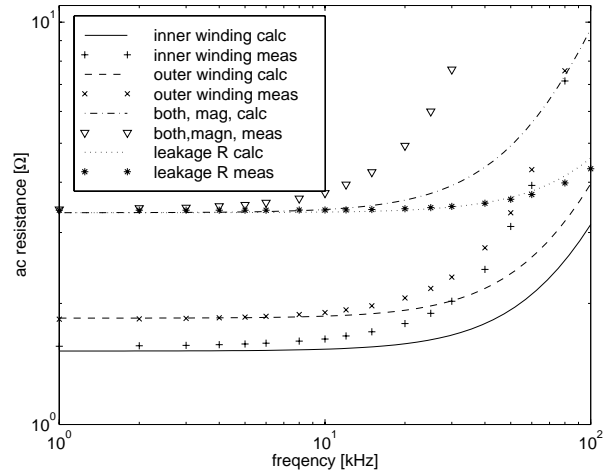


Fig. 4. Real part of the impedance of various winding configurations for the gapped-ferrite-core transformer, compared to the predicted ac resistance.

resonant frequencies we measure (see Table II), which correspond to self capacitance of around 200 pF. In all cases, the discrepancies only become significant as the self-resonant frequency is approached. (For example, with the “leakage inductance” connection, the self-

TABLE II
WINDING RESONANT FREQUENCIES

Winding	f_0 , air core	f_0 , gapped ferrite core
inner	762 kHz	196 kHz
outer	752 kHz	193 kHz
both—magnetizing	392 kHz	100 kHz
both—leakage	1552 kHz	841 kHz

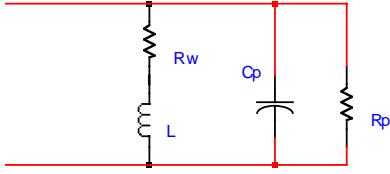


Fig. 5. Circuit representing winding impedance.

resonant frequencies are very high, and the results match well with no correction.) To account for those effects, the model shown in Fig. 5 was used. Here, C_p represents winding capacitance and R_p represents dielectric loss in this capacitance. The real part of the impedance of this network, R_m is what is measured. However, R_w is what is predicted by the analysis. To resolve this, we found values for C_p and R_p and then corrected the measurements to obtain experimental values for R_w that could be compared to our predictions, using the relationship

$$R_m = \text{Re} \left\{ (R_w + j\omega L) \parallel \left(R_p \parallel \frac{1}{j\omega C_p} \right) \right\}, \quad (9)$$

where $\text{Re}\{\cdot\}$ indicates the real part. This expression was solved for R_w . Values for C_p were calculated from the self-resonant frequency of each winding or winding combination. Values for R_p were obtained by measuring loss with a closed core and the actual winding driven with the same voltage as in the winding resistance test. These measurements included both winding capacitive loss and core loss, and so could be used for the gapped-core test directly, without additional compensation for the core loss. However, for the air-core case, the core loss had to be subtracted from the new measurement to obtain a measurement that represented just dielectric loss.

The capacitance corrections were much more significant than the core-loss corrections. The corrected data is shown in Figs. 6 and 7. In these plots the predictions match very closely, given the multiple opportunities for error introduced by the multiple steps in correction process.

D. Discussion

To the best of our ability to isolate ac winding loss from other effects, our predictions match the experimental results. However, measurements on additional transformers with lower self-capacitance, such that that corrections for capacitive effects are not required, are planned. This will allow greater confidence in the measurements, and allow more precise comparisons between calculation and measurement.

The comparison with predictions from one-dimensional analysis in Fig. 7 shows dramati-

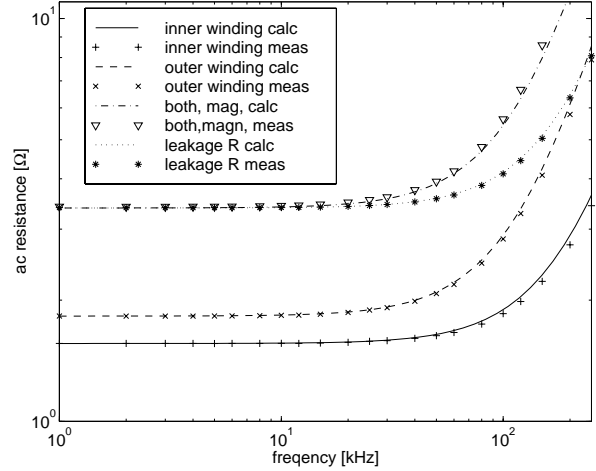


Fig. 6. Measured ac resistance of various winding configurations for the tested air-core coil, as corrected using (9), compared to the predicted ac resistance.

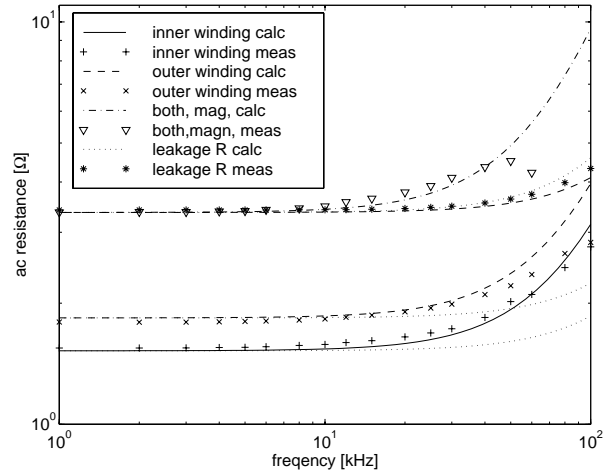


Fig. 7. Measured ac resistance of various winding configurations for the tested gapped-ferrite-core transformer, as corrected using (9), compared to the predicted ac resistance. Also show as dotted lines are the ac resistance factors for the individual windings predicted by one-dimensional analysis. Because, for two windings in series, one-dimensional analysis predicts the same resistance for either connection, one line (dashed) represents the predicted resistance for both configurations.

ically the improvement in accuracy afforded by the new method.

Addressing accurate prediction of loss in windings that are operating in or near self resonance could also be of interest. In self resonance, the current is different in each turn in the winding, and so the field geometry and proximity effect losses can change significantly. Our model (Fig. 5) does not attempt to include these effects. However, this is of less practical value, since a large self capacitance will, in most applications, lead to high circuit losses and EMI and so should be avoided in the design anyway.

E. Computational Costs

The predictions were obtained with quite modest computational costs. A comparison with a direct simulation was not possible, as the computational cost would have been prohibitive. However, we performed such a comparison with a simpler design. We compared the two-dimensional magnetostatic simulation required for our method to a full two-dimensional simulation of strand eddy currents in a 250 kHz inductor with 110 turns of 0.4 mm diameter wire. The magnetostatic analysis required for our method took six seconds, whereas the full eddy-current analysis took over 18 minutes. Using a device with only 110 strands, as opposed to the 2500 strands in our experimental device made this experiment possible, but also minimized the difference in simulation time¹. The difference would be even more dramatic for more complex structures, for more strands, or for three-dimensional simulations. The test was based on the assumption of a sinusoidal current waveform. Non-sinusoidal waveforms would require no additional magnetostatic simulation time for our method, but, for the full finite-element analysis of eddy currents, would require an additional, similar simulation for each harmonic.

V. ASSUMPTIONS AND SCOPE OF APPLICATION

The method presented here allows analysis of a wider range of winding types than do previous methods; it allows both arbitrary waveforms and two- or three-dimensional field geometries. However, there are a number of assumptions that have been made in the analysis. Most of these were noted in the derivation; we repeat them here for clarification of how they limit the scope of the method.

The analysis is based on round wires. Other shapes could be analyzed by similar methods, as long as all the dimensions were small compared to the winding window. However, the loss will then depend on the the orientation of the field, somewhat complicating calculations. In the case of litz wire, we have assumed that bundle-level effects are negligible, a valid assumption for well-designed litz constructions [21]. We have also assumed that the wire (or strand, in the case of litz wire) is small compared to a skin depth. If it is not, a similar approach could be used, combining magnetostatic field calculations with slightly more complicated analysis of the loss in the winding, such as that in [6, 18]. For such situa-

¹Both simulations used the same two-dimensional finite-element simulation package (Ansoft Maxwell) with adaptive mesh refinement and a 1% energy error criterion, running on a 300 MHz Pentium machine. The magnetostatic simulation was completed in six seconds, using less than one second of CPU time, whereas the full simulation took over 18 minutes of CPU time. Memory requirements were 1 MB and 16 MB respectively.

tions, it may also be necessary to modify the magnetostatic analysis to account for the effect the winding has on the field distribution.

If two-dimensional field calculations are used, this entails a degree of approximation that depends on the importance of three-dimensional effects in the particular geometry under study. However, three-dimensional calculations may also be used. This still entails a minor approximation: The loss induced by a field parallel to the axis of the wire is less than the loss we calculate assuming a perpendicular field. In most geometries of interest, the parallel component of the field is small. If it were significant, this would lead to a slightly conservative prediction of loss.

As discussed above in Section IV, capacitive effects can change the current distribution in the winding, making the field calculation invalid. Thus, the method is not directly applicable for windings in or near self-resonance.

Finally, we also note that the use of a magnetostatic field calculation is implicitly based on the assumption that hysteresis in the core does not significantly affect the field in the window area. Such an effect would only happen with extremely high hysteresis loss, and so is not likely to be a problem in any power applications. (The hysteresis loss would need to be high compared to the VA handled by the inductor or transformer, not just compared to other losses.)

In summary, most of the assumptions discussed above are nearly always valid, except for one: that the winding is constructed with round wire that is small compared to a skin depth.

VI. CONCLUSION

The method described above allows calculating losses in multi-winding transformers with two- and three-dimensional field effects and arbitrary waveforms in each winding. It uses a simple set of magnetostatic field calculations to derive a matrix describing the transformer. This is combined with a second matrix calculated from derivatives of winding currents to calculate total ac loss. Experiments show the method is accurate for coils that are not in or close to self-resonance.

The method makes it possible to calculate loss using only computationally inexpensive magnetostatic field calculations for situations that previously would have required numerical eddy-current simulations that are computationally prohibitive. The increase in speed not only can make it easier to predict loss for a given design, but also can make numerical optimization practical. In addition, the way many parameters affect loss is made explicit. These explicit relationships are expected to be useful in analytical optimizations of some aspects of the winding and component design.

VII. ACKNOWLEDGMENT

Thanks to West Coast Magnetics for winding test transformers, including rapid replacement of a transformer we accidentally stepped on.

REFERENCES

- [1] S. Butterworth, "Effective resistance of inductance coils at radio frequency – part i", *The Wireless Engineer*, vol. 3, pp. 203–210, Apr. 1926.
- [2] S. Butterworth, "Effective resistance of inductance coils at radio frequency – part ii", *The Wireless Engineer*, vol. 3, pp. 309–316, May 1926.
- [3] S. Butterworth, "Effective resistance of inductance coils at radio frequency – part iii", *The Wireless Engineer*, vol. 3, pp. 417–424, July 1926.
- [4] S. Butterworth, "Effective resistance of inductance coils at radio frequency – part iv", *The Wireless Engineer*, vol. 3, pp. 483–492, Aug. 1926.
- [5] G.W.O. Howe, "The high-frequency resistance of multiply-stranded insulated wire", *Proceedings of the Royal Society of London*, vol. XCII, pp. 468–492, Oct. 1917.
- [6] J. A. Ferreira, "Improved analytical modeling of conductive losses in magnetic components", *IEEE Transactions on Power Electronics*, vol. 9, pp. 127–31, Jan. 1994.
- [7] P.L. Dowell, "Effects of eddy currents in transformer windings", *Proceedings of the IEE*, vol. 113, pp. 1387–1394, Aug. 1966.
- [8] J. Jongsma, "Minimum loss transformer windings for ultrasonic frequencies, part 1: Background and theory", *Phillips Electronics Applications Bulletin*, vol. E.A.B. 35, pp. 146–163, 1978.
- [9] J. Jongsma, "Minimum loss transformer windings for ultrasonic frequencies, part 2: Transformer winding design", *Phillips Electronics Applications Bulletin*, vol. E.A.B. 35, pp. 211–226, 1978.
- [10] J. Jongsma, "High frequency ferrite power transformer and choke design, part 3: Transformer winding design", Technical Report 207, 1986.
- [11] P. S. Venkatraman, "Winding eddy current losses in switch mode power transformers due to rectangular wave currents", in *Proceedings of Powercon 11*, pp. 1–11. Power Concepts, Inc., 1984.
- [12] N. R. Coonrod, "Transformer computer design aid for higher frequency switching power supplies", in *IEEE Power Electronics Specialists Conference Record*, pp. 257–267, 1984.
- [13] J. P. Vandelac and P. Ziogas, "A novel approach for minimizing high frequency transformer copper losses", in *IEEE Power Electronics Specialists Conference Record*, pp. 355–367, 1987.
- [14] Lloyd H. Dixon Jr., "Review of basic magnetics. theory, conceptual models, and design equations", in *Unitrode Switching Regulated Power Supply Design Seminar Manual*, pp. M4–1 to M4–11. Unitrode Corporation, 1988.
- [15] E. C. Snelling, *Soft Ferrites, Properties and Applications*, Butterworths, second edition, 1988.
- [16] Audrey M. Urling, Van A. Niemela, Glenn R. Skutt, and Thomas G. Wilson, "Characterizing high-frequency effects in transformer windings—a guide to several significant articles", in *APEC 89*, pp. 373–385, Mar. 1989.
- [17] J. A. Ferreira, *Electromagnetic Modelling of Power Electronic Converters*, Kluwer Academic Publishers, 1989.
- [18] William R. Smythe, *Static and Dynamic Electricity*, McGraw-Hill, 1968, page 411.
- [19] P. N. Murgatroyd, "The toroidal cage coil", *IEE Proceedings, Part B*, vol. 127, pp. 207–214, 1980.
- [20] Sergio Crepaz, "Eddy-current losses in rectifier transformers", *IEEE Transactions on Power Apparatus and Systems*, vol. PAS-89, pp. 1651–1662, 1970.
- [21] Charles R. Sullivan, "Optimal choice for number of strands in a litz-wire transformer winding.", *IEEE Transactions on Power Electronics*, vol. 14, pp. 283–291, 1999.
- [22] J. M. Lopera, M. J. Prieto, F. Nuno, A. M. Pernia, and J. Sebastian, "A quick way to determine the optimum layer size and their disposition in magnetic structures", in *28th Annual IEEE Power Electronics Specialists Conference*, pp. 1150–1156, 1997.
- [23] J.G. Breslin and W.G. Hurley, "Derivation of optimum winding thickness for duty cycle modulated current waveshapes", in *28th Annual IEEE Power Electronics Specialists Conference*, vol. 1, pp. 655–661, 1997.
- [24] Rudy Severns, "Additional losses in high frequency magnetics due to non ideal field distributions", in *Seventh Annual IEEE Applied Power Electronics Conference*, pp. 333–8, 1992.
- [25] Peter Wallmeier, N. Frohleke, and H. Grotstollen, "Improved analytical modeling of conductive losses in gapped high-frequency inductors", in *Proceedings of the 1998 IEEE Industry Applications Society Annual Meeting*, pp. 913–920, 1998.
- [26] Jiankun Hu and Charles R. Sullivan, "Optimization of shapes for round-wire high-frequency gapped-inductor windings", in *Proceedings of the 1998 IEEE Industry Applications Society Annual Meeting*, pp. 900–906, 1998.
- [27] Jiankun Hu and C. R. Sullivan, "The quasi-distributed gap technique for planar inductors: Design guidelines", in *Proceedings of the 1997 IEEE Industry Applications Society Annual Meeting*, pp. 1147–1152, 1997.
- [28] Ansoft Corporation, *Maxwell, Finite Element Analysis Software*, Pittsburgh, Pennsylvania, USA, <http://www.ansoft.com>.